



HAL
open science

Impact of the saturable absorber on the linewidth enhancement factor of hybrid silicon quantum dot comb lasers (Student paper)

Thibaut Renaud, Heming Huang, Geza Kurczveil, R G Beausoleil, Frédéric Grillot

► **To cite this version:**

Thibaut Renaud, Heming Huang, Geza Kurczveil, R G Beausoleil, Frédéric Grillot. Impact of the saturable absorber on the linewidth enhancement factor of hybrid silicon quantum dot comb lasers (Student paper). 2023 European Conference on Integrated Optics (ECIO), Apr 2023, Twente, Netherlands. hal-04559961

HAL Id: hal-04559961

<https://telecom-paris.hal.science/hal-04559961>

Submitted on 25 Apr 2024

HAL is a multi-disciplinary open access archive for the deposit and dissemination of scientific research documents, whether they are published or not. The documents may come from teaching and research institutions in France or abroad, or from public or private research centers.

L'archive ouverte pluridisciplinaire **HAL**, est destinée au dépôt et à la diffusion de documents scientifiques de niveau recherche, publiés ou non, émanant des établissements d'enseignement et de recherche français ou étrangers, des laboratoires publics ou privés.

Impact of the saturable absorber on the linewidth enhancement factor of hybrid silicon quantum dot comb lasers

(Student paper)

Thibaut Renaud^{1*}, Heming Huang¹, Geza Kurczveil², R.G. Beausoleil² and Frédéric Grillot^{1,3}

¹LTCI, Télécom Paris, Institut Polytechnique de Paris, 19 place Marguerite Perey, 91120 Palaiseau, France

²Large-Scale Integrated Photonics Lab, Hewlett Packard Labs, Hewlett Packard Enterprise, Milpitas, CA 95035, USA

³Center for High Technology Materials, University of New-Mexico, 1313 Goddard SE, Albuquerque, USA

*correspondence to: thibaut.renaud@telecom-paris.fr

This work investigates the effects of the saturable absorber on the linewidth enhancement factor of hybrid silicon quantum dot comb lasers, which is a key parameter involved in frequency comb generation. Experiments have been performed on two carefully chosen laser devices sharing the same gain material and cavity design, with and without saturable absorber. The results unveil that the increase of the reversed bias on the absorber drives up the linewidth enhancement factor, which gives birth to the comb spectrum. This paper brings insights on the fundamental aspects of comb lasers and provides concepting guidelines of future on-chip light sources for integrated wavelength-division multiplexing applications.

Keywords: Quantum dots, frequency combs, linewidth enhancement factor, silicon photonics

INTRODUCTION

The recent years have seen a great increase in data transfer for smaller and smaller distances, in particular for High Performance Computing (HPC) systems where it reaches several petabits per second between the memory and the different compute nodes¹. These optical interconnects rely on on-chip wavelength-division multiplexing (WDM) to transmit the data through multiple separately modulated channels at once, in order to vastly improve the transfer speed. Although this approach can be achieved using one single-wavelength laser per channel, it is not very suitable for silicon based integrated photonics circuits (PICs) as it results in a larger footprint and energy consumption. On top of that, it is also associated to a lower stability since WDM requires all modes frequencies to stay equally spaced. Therefore, a better solution consists in using a single laser with a quantum dot (QD) active region producing an efficient optical frequency comb (OFC) wherein the phase of each line cannot shift independently from the others². Furthermore, the ultimate carrier quantization within the QDs provides lasers with an exceptional thermal stability, along with a large gain bandwidth and a narrow linewidth³ which is desired in OFC. On the first hand, the linewidth of each comb line is linked to the phase noise and can be reduced through the linewidth enhancement factor (α_H -factor), while on the other hand, the operating comb bandwidth directly scales with the magnitude of α_H -factor^{4,5}. As a consequence of that, the optimization of the comb properties requires a careful understanding of the α_H -factor in particular, when a saturable absorber (SA) is incorporated in the device. In this work, we are experimentally looking at this concern in two hybrid silicon InAs/GaAs QD comb lasers. The lasers share the same gain material, but possess slightly different cavity designs hence one has a SA section and the other does not. We believe that this paper brings further insights on comb lasers which is of paramount importance for future on-chip light sources for integrated WDM applications in data centers and in supercomputers.

LASER STRUCTURE

The multi-section cavity design of the devices is shown schematically in Figure 1(a). The structure consists of a 2.6-mm-long cavity that has mirrors with 50% reflectivity on one side and 100% on the other, and a 1.4-mm-long active region is placed in the center. The semiconductor optical amplifier (SOA) section incorporates 8 layers of QDs, and one of the two lasers has a 176- μm -long SA positioned in the middle in order to favor the frequency comb operation. Mode converters ensure the optical mode transfer from active waveguide down to the passive Si waveguide and the output light is coupled out through a grating coupler (GC).

The integration on silicon is realized by wafer-bonding an unpatterned InAs/GaAs QD wafer to a Silicon-on-Insulator (SOI) wafer already patterned with the Si passive devices. The QD material is then etched and the p- and n-contacts are deposited, using standard III-V processing techniques. More information about the epitaxial structure can be found elsewhere^{6,7}.

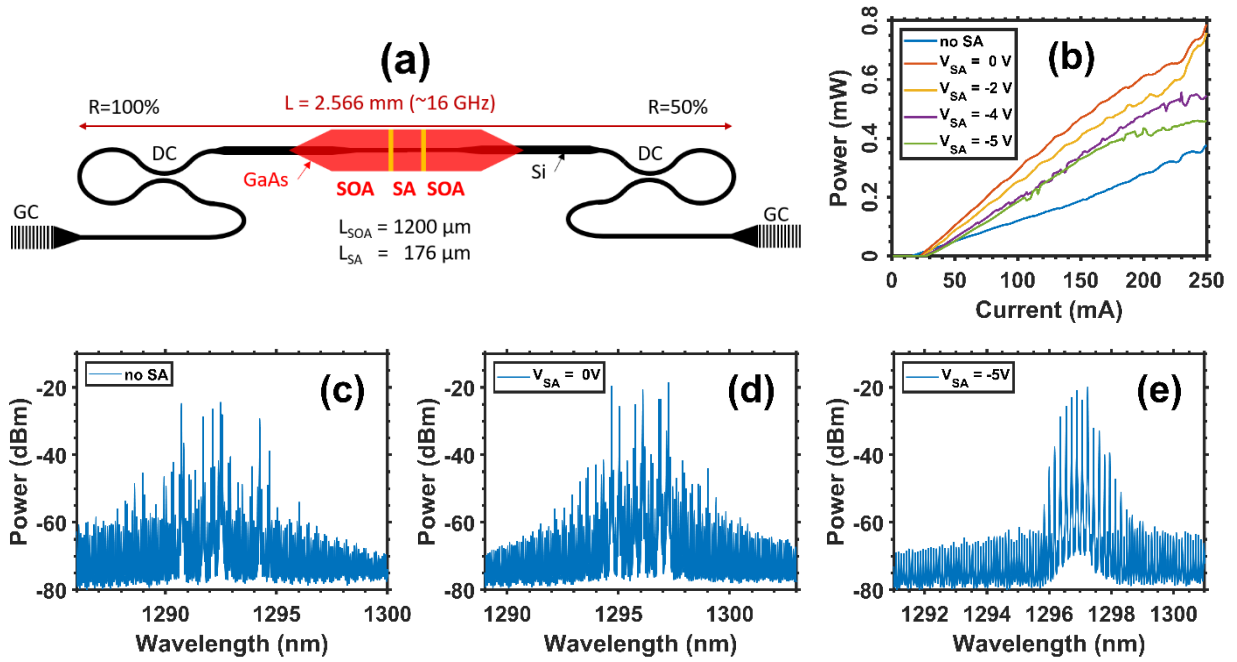


Fig. 1. (a) Schematics of the laser design. SOA: semiconductor optical amplifier; SA: saturable absorber; GC: Grating Coupler; DC: directional coupler. (b) LI characteristics of the two lasers at 20°C . (c)(d)(e) Optical spectra of the two lasers at $2 \times I_{th}$ and 20°C .

Figure 1(b) shows the LI characteristics of both lasers at room temperature (20°C), with applied voltages of $V_{\text{SA}} = 0 \text{ V}$, -2 V , -4 V and -5 V for the SA. The threshold current I_{th} increases from 23 mA to 27 mA when the SA voltage goes from 0V to -5V, while the laser without SA has a threshold at 16 mA. The higher threshold is due to the increased internal loss coefficient in the SA. The optical spectra depicted in Figure 1(c), (d) and (e) show the evolution of the frequency comb at room temperature (20°C) for the laser without SA and for the other one at $V_{\text{SA}} = 0 \text{ V}$ and -5 V . Both lasers are pumped at $2 \times I_{th}$. Under these conditions, the emission wavelength is centered around 1292 nm, 1296 nm and 1297 nm, respectively. At a -5 V reverse voltage condition, the comb spectrum takes place with 15 lines above noise floor, and with 6 lines within the -10 dB bandwidth.

RESULTS AND DISCUSSION

The impact of the SA on the α_H -factor of the laser can be better understood by tracking the modal wavelength shift below threshold. The α_H -factor has often been measured in mono-section devices under straightforward biased condition whereas for reverse biased SAs it has not been extensively studied or measured despite the importance to understand its magnitude in SAs. The α_H -factor is measured from the Amplified Spontaneous Emission (ASE)⁸⁻¹¹. Its extraction is performed by capturing a set of optical spectra below and above the laser's threshold with a high-resolution (10 pm) optical spectrum analyzer (OSA), and then by calculating the differential gain $\Delta g/\Delta I$ and the wavelength shift $\Delta\lambda/\Delta I$ for each longitudinal mode. A correction for the thermal red-shift is taken into account using the above threshold spectra¹⁰. Finally, the α_H of each comb line is retrieved through the expression^{8,10,11}

$$\alpha_H = -\frac{4n\pi}{\lambda^2} \frac{\Delta\lambda/\Delta I}{\Delta g/\Delta I} \quad (1)$$

where n is the effective group index, λ the photon wavelength, and g the net modal gain.

Figure 2(a) shows the wavelength shift $\Delta\lambda$ with respect to the normalized current I/I_{th} for one mode in each laser. Without SA, the wavelength is found slightly blue-shifted below threshold and red-shifted above due to thermal effects. However, when the SA is included (assuming $V_{\text{SA}} = 0 \text{ V}$), the wavelength is found redshifted with increasing the pump current even from below threshold. This thermal load is also retrieved at any other reverse voltage conditions. Therefore, the saturation of the absorber is connected with the thermal heating of the device.

Figure 2(b) displays the threshold value of the linewidth enhancement factor for each condition on the SA studied in this work. This value is taken as the mean of the α_H -factors of a few modes around the first lasing mode, which is to say the mode with the highest intensity just above threshold. As the two lasers have the same design, the difference in the α_H -factor is only due to the presence of the SA. First, the orange triangle represents the laser

without SA. Therefore, the measured value at 0.9 reflects the α_H of the sole nominal gain section. In the open circuit (OC) configuration, the laser with SA exhibits a α_H -factor of around 1, hence slightly higher than the one without. At higher reverse voltages, it slightly goes up monolithically until a sharp increase occurs around -4V, up to ~ 2.5 for $V_{SA} = -5V$. This threshold effect is concomitant with the birth of the comb lines displayed in Figure 1(c). Note that this phenomenon has already been observed in other similar devices⁴. This result somewhat illustrates the interplay between this device parameter governing many coherent processes in semiconductor lasers, and the frequency comb operation.

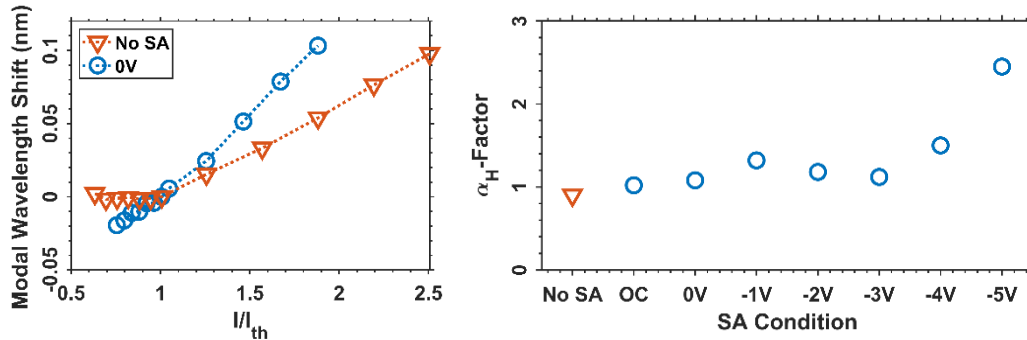


Fig. 2. (a) Wavelength shift $\Delta\lambda$ with respect to the normalized current I/I_{th} for the laser without SA and for the laser with SA at $V_{SA} = 0V$. (b) The mean value of the α_H -factor for a few modes around the first lasing mode at different SA conditions. OC: open circuit.

CONCLUSION

In this work, the influence of the SA on the linewidth enhancement factor is studied in multi-section hybrid silicon QD lasers. The experiments unveil that, the introduction of the SA enhances the α_H -factor of the device especially when the comb spectrum is formed at higher reverse bias conditions. Here, we present an experimental demonstration of a QD comb laser, confirming the predicted key role of the α_H -factor in the formation of the frequency comb dynamics. These results gained deeper insights on the underlying physics of multi-section comb lasers and thus provide further guidelines for the conception of future on-chip multi-wavelength light sources in integrated WDM applications.

Acknowledgements: This work is supported by Hewlett Packard Enterprise (HPE) and the Institut Mines Telecom.

References

- [1] D. Dai and J. E. Bowers, *Silicon-based on-chip multiplexing technologies and devices for peta-bit optical interconnects*, *Nanophotonics* **3**(4-5), pp. 283–311, 2014.
- [2] L. Lundberg, M. Karlsson, A. Lorences-Riesgo, M. Mazur, V. Torres-Company, J. Schröder, and P. A. Andrekson, *Frequency comb-based wdm transmission systems enabling joint signal processing*, *Applied Sciences* **8**(5), 2018.
- [3] J. Duan, H. Huang, Z. G. Lu, P. J. Poole, C. Wang, and F. Grillot, *Narrow spectral linewidth in inas/inp quantum dot distributed feedback lasers*, *Applied Physics Letters* **112**(12), p. 121102, 2018.
- [4] B. Dong, H. Huang, J. Duan, G. Kurczveil, D. Liang, R. G. Beausoleil, and F. Grillot, *Frequency comb dynamics of a 1.3 μm hybrid-silicon quantum dot semiconductor laser with optical injection*, *Opt. Lett.* **44**, 5755-5758, 2019.
- [5] F. Cappelli, G. Villares, S. Riedi, and J. Faist, *Intrinsic linewidth of quantum cascade laser frequency combs*, *Optica* **2**, 836-840, 2015.
- [6] G. Kurczveil, A. Descos, D. Liang, M. Fiorentino, and R. Beausoleil, *Hybrid silicon quantum dot comb laser with record wide comb width*, in *Frontiers in Optics / Laser Science*, p. FTu6E.6, Optical Society of America, 2020.
- [7] G. Kurczveil, D. Liang, M. Fiorentino, and R. G. Beausoleil, *Robust hybrid quantum dot laser for integrated silicon photonics*, *Opt. Express* **24**, pp. 16167–16174, 2016.
- [8] H. Huang, K. Schires, P. J. Poole, and F. Grillot, *Non-degenerate four-wave mixing in an optically injection-locked InAs/InP quantum dot Fabry–Perot laser*, *Appl. Phys. Lett.* **106**, p. 143501, 2015.
- [9] C. Wang, F. Grillot, F. Y. Lin, I. Aldaya, T. Batte, C. Gosset, E. Decerle, and J. Even, *Nondegenerate Four-Wave Mixing in a Dual-Mode Injection-Locked InAs/InP(100) Nanostructure Laser*, *IEEE Photonics Journal*, vol. **6**, no. 1, pp. 1-8, 2014.
- [10] B. Zhao, T. R. Chen, S. Wu, Y. H. Zhuang, Y. Yamada, and A. Yariv, *Direct measurement of linewidth enhancement factors in quantum well lasers of different quantum well barrier heights*, *Appl. Phys. Lett.* **62**, 1591-1593, 1993.
- [11] R. Raghuraman, N. Yu, R. Engelmann, H. Lee and C. L. Shieh, *Spectral dependence of differential gain, mode shift, and linewidth enhancement factor in a InGaAs-GaAs strained-layer single-quantum-well laser operated under high-injection conditions*, in *IEEE Journal of Quantum Electronics*, vol. **29**, no. 1, pp. 69-75, 1993.